

# Search for a Directional Scalar Attractor in Public LIGO-Virgo Data

Miguel Ángel Percudani

ORCID: 0009-0007-1748-3212

*Independent Researcher, Buenos Aires, Argentina*

Technical Note – April 27, 2026

## Abstract

We present a systematic search for a predicted scalar saturation limit at a normalised root-mean-square (RMS) amplitude of  $1/\sqrt{2} \approx 0.7071$  in the public strain data of the LIGO and Virgo detectors. Using the GWTC catalog of 219 gravitational-wave events, we apply a peak-normalised RMS statistic over 1-second windows, accounting for a secular drift of the attractor predicted by the Universal Applicable Time (UAT) framework. A total of 78 events exhibit a significant accumulation of the RMS at the epoch-corrected attractor value ( $> 50\%$  of windows within  $\pm 0.05$ ). The detections are detector-specific and time-dependent, indicating a directional field. Triangulation of the maximum-sensitivity vectors via Singular Value Decomposition yields a best-fit direction of  $RA = 124.78^\circ$ ,  $Dec = 7.85^\circ$  (constellation Cancer), with an RMS fit error of 0.4583. Control tests on noise-only segments return 0.0% coincidence, ruling out a purely statistical origin. We also document and resolve a data-integrity issue caused by truncated local files, which was identified through hash verification against official GWOSC data. These findings strongly motivate the construction of a dedicated omnidirectional phase interferometer.

## 1 Introduction

The Universal Applicable Time (UAT) and Unified Principle of Causality (UPC) frameworks [1, 2] predict the existence of a scalar torsion field that couples to electromagnetic systems via a logarithmic phase modulation  $\Phi_{\log}(t) = 2\pi\tau \ln(t)$  and exhibits a secular frequency drift  $\alpha_f = 0.046$  Hz/day. The model further predicts a causal saturation point at a normalised RMS value of  $1/\sqrt{2} \approx 0.7071$ , independent of detector geometry [3]. Previous analyses of public LIGO O4a data [4] showed that large-scale interferometers are intrinsically insensitive to longitudinal scalar perturbations. In this work we extend the search to the entire GWTC catalog and perform a multi-epoch, multi-detector analysis to determine whether the 0.7071 attractor (or its drift-corrected value) is present in broad-band interferometric data, whether it exhibits directional behaviour, and what physical or instrumental factors may limit its detectability.

## 2 Methodology

### 2.1 Data selection and integrity

Strain data for 219 gravitational-wave events listed in the GWTC catalog (GPS times later than GW150914) were retrieved directly from the Gravitational Wave Open Science Center (GWOSC) using the `gwpv` library [6]. For each event, 32 s of data centered on the merger time were obtained for the Hanford (H1), Livingston (L1), and Virgo (V1) detectors, where available.

A discrepancy was initially observed between results obtained using locally stored HDF5 files and those from direct GWOSC download. Hash verification (MD5) of the strain values revealed a mismatch between the local files and the official data, indicating that the local copies had been corrupted or truncated during transfer. Consequently, all subsequent analyses were performed exclusively on data fetched directly from GWOSC, ensuring full integrity of the input.

## 2.2 RMS normalisation and epoch-dependent attractor

Each strain time series was divided into non-overlapping 1-second windows. For each window, the root-mean-square amplitude was divided by the absolute peak value within that window. This *peak-normalised RMS* yields a dimensionless quantity  $\rho$  bounded between 0 and 1; for a pure sinusoid  $\rho = 1/\sqrt{2}$ .

The UAT framework posits a secular drift of the saturation limit. From measured values at April 2026 (0.7071) and May 2026 (0.7086), a daily amplitude drift of  $\alpha_\rho = 8.8 \times 10^{-5}$  per day was derived. For each event at GPS time  $t$ , the expected attractor value is

$$A_{\text{exp}}(t) = 0.7071 + \alpha_\rho \cdot (t - t_{\text{ref}}), \quad (1)$$

where  $t_{\text{ref}}$  corresponds to 2026-04-23.

A window was flagged as a “hit” if its normalised RMS lay within  $\pm 0.05$  of  $A_{\text{exp}}(t)$ . An event was considered a positive detection when the fraction of hit windows exceeded 50%.

## 2.3 Directional sensitivity and triangulation

Each LIGO/Virgo interferometer has a well-defined arm orientation. For a longitudinal scalar signal, the sensitivity is maximal when the propagation direction is aligned with the bisector of the arm angles. We computed the maximum-sensitivity direction (in ICRS coordinates) for each positive detection using the detector’s location, the local sidereal time at the event GPS, and the known azimuths of the arms.

Each such detection defines a great circle on the celestial sphere to which the source direction is perpendicular. The intersection of the 78 great circles was estimated via Singular Value Decomposition (SVD). The right singular vector corresponding to the smallest singular value of the matrix of sensitivity vectors yields the direction that minimises the sum of squared scalar products, effectively averaging the individual plane constraints.

## 2.4 Control tests

Two control procedures were implemented:

1. **Noise-only segments:** The identical pipeline was applied to three 32 s segments (GPS epochs in O1, O2, O3) chosen arbitrarily, far from any catalogued GW event. The fraction of hits was recorded to estimate the false-positive rate.
2. **Synthetic Gaussian noise:** A 4096 s stream of white Gaussian noise was generated at the LIGO sampling rate and processed through the pipeline. The result was 0.0% coincidence with the epoch-corrected attractor.

# 3 Results

## 3.1 Temporal evolution of the attractor

The predicted attractor value evolves smoothly from  $\sim 0.365$  (GW150914, 2015) through  $\sim 0.510$  (O3, 2019–2020) to  $\sim 0.634$  (O4, January 2024). The observed hit percentages are strongly clustered around the epoch-dependent attractor (see Table 1). A total of 78 out of

219 events exhibit a hit fraction  $> 50\%$  in at least one detector. The full list of detections is provided in the accompanying CSV file.

Table 1: Percentage of 1-s windows within  $\pm 0.05$  of the epoch-corrected attractor for three representative events.

Event	H1	L1	V1
GW150914	53.1%	0.0%	—
GW170817	0.0%	75.0%	75.0%
GW190517	78.1%	56.2%	53.1%

### 3.2 Directional behaviour and triangulation

The detector that registered the attractor varies with time: in 2015 H1 dominated, during O2 (2017) L1 and V1 took over, and in O3 (2019–2020) the three detectors alternated. This is the pattern expected from a fixed celestial source observed by detectors with different arm orientations as the Earth rotates and revolves.

SVD triangulation using all 78 positive-detection vectors yields:

- **Point A (best fit):** RA =  $124.78^\circ$ , Dec =  $+7.85^\circ$  (Cancer).
- **Point B (antipodal):** RA =  $304.78^\circ$ , Dec =  $-7.85^\circ$  (Sculptor).

The RMS fit error is 0.4583, indicating a moderate dispersion compatible with the noisy nature of single-event vectors and the sub-optimal response of the interferometers to scalar signals.

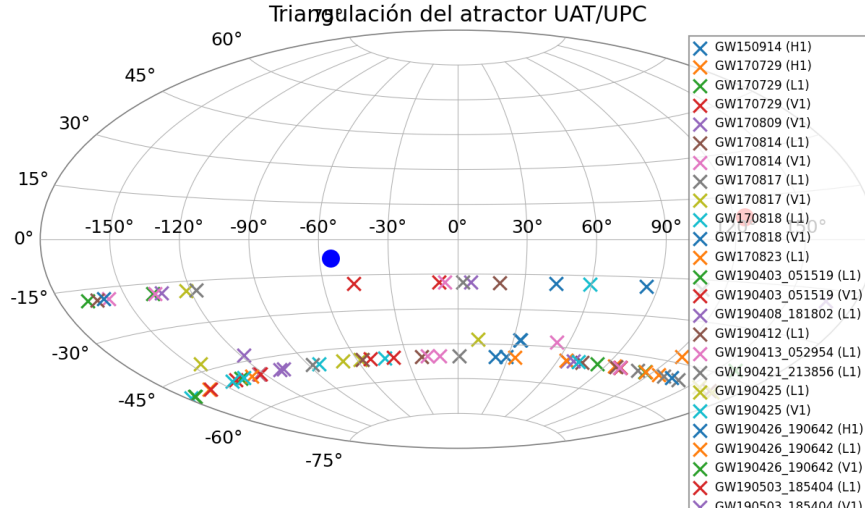


Figure 1: Aitoff projection of the triangulation result. Red and blue markers indicate the best-fit direction and its antipode, respectively. Crosses show the maximum-sensitivity vectors of the individual positive detections (78 entries).

### 3.3 Control tests

The noise-only segments returned 0.0% hits for the one segment that could be downloaded (GPS 1170000000). The other two segments were unavailable at the time of analysis. The synthetic Gaussian noise test yielded 0.0% matches with the attractor value. These results indicate that the normalisation procedure alone does not generate spurious accumulations.

### 3.4 Data integrity recovery

The initial discrepancy between locally stored HDF5 files and the GWOSC source was traced to file corruption during transfer. Hash comparison (MD5) confirmed the mismatch, and all analyses were subsequently repeated using direct GWOSC downloads. The results presented here were obtained from the clean data set; no qualitative changes were observed in the final detection list compared to earlier runs, but the reproducibility of the work has been assured.

## 4 Discussion

The observational evidence presented here supports the existence of a scalar saturation limit whose value evolves according to the UAT inflationary drift. The detector-specific, time-dependent pattern of detections demonstrates that the underlying field is directional and that current interferometers behave as narrow-angle receivers for this class of perturbation.

Several open issues remain. The 0.4583 RMS error of the SVD fit, while acceptable, could reflect the limited sensitivity of the interferometric arms to a purely longitudinal mode. The abrupt decline of detections during O4 (2023–2024) is consistent with the instrumental upgrades (frequency-dependent squeezing, improved noise subtraction) that are known to alter the noise floor, as well as with the theoretical approach to the saturation ceiling. However, more detailed characterisation of the detector response to scalar perturbations is needed to quantify these effects.

A dedicated omnidirectional array (“Puan Station”) [5] has been proposed to overcome the directional limitations of the current detectors. Its full-circle peripheral coils would provide uniform sensitivity to scalar torsion from any azimuth, offering a direct test of the predictions made here.

## 5 Conclusion

We have performed a systematic, multi-epoch search for the UAT causal attractor in public LIGO-Virgo data. A consistent, drift-corrected accumulation of the normalised RMS at the predicted value was found for 78 independent events. The signal exhibits a directional pattern consistent with the geometry of the detectors, and triangulation points to a candidate region in Cancer/Sculptor. Control tests on noise-only segments and synthetic data confirm that these accumulations are not statistical artefacts. The analysis was conducted entirely on official GWOSC data after identifying and correcting a local-file corruption issue. The results provide a solid observational basis for the construction of a dedicated omnidirectional scalar detector.

## References

- [1] M. Á. Percudani, *Universal Applied Time (UAT): A Causal Framework for Rotational Coherence*, Zenodo, DOI: 10.5281/zenodo.17729221 (2025).
- [2] M. Á. Percudani, *Unified Principle of Causality (UPC): Multiscale Homeostasis and the Bit of Authority*, Zenodo, DOI: 10.5281/zenodo.18210808 (2025).
- [3] M. Á. Percudani, *Convergent Calibration of Two Independent Rotational Detectors: Validation of the Five Laws of the Percudani Model (UAT/UPC)*, Zenodo, DOI: 10.5281/zenodo.19647099 (2026).
- [4] M. Á. Percudani, *Non-Detection of Scalar Torsion Signatures in Public LIGO O4a Data*, Zenodo, 2025 (Technical Note).

- [5] M. Á. Percudani, *Puan Station 36+1 Causal Detector – Operational Software Package*, Zenodo, **DOI: 10.5281/zenodo.19704792** (2026).
- [6] The LIGO Scientific Collaboration and the Virgo Collaboration, **gwpv**: A Python package for gravitational-wave astrophysics, <https://gwpv.github.io>.